



HAL
open science

Phase control of transmission and reflection in a sample of duplicated two-level systems driven by a stationary control field

F A Hashmi, E. Brion, M A Bouchene

► **To cite this version:**

F A Hashmi, E. Brion, M A Bouchene. Phase control of transmission and reflection in a sample of duplicated two-level systems driven by a stationary control field. 2024. hal-04605029

HAL Id: hal-04605029

<https://hal.science/hal-04605029>

Preprint submitted on 7 Jun 2024

HAL is a multi-disciplinary open access archive for the deposit and dissemination of scientific research documents, whether they are published or not. The documents may come from teaching and research institutions in France or abroad, or from public or private research centers.

L'archive ouverte pluridisciplinaire **HAL**, est destinée au dépôt et à la diffusion de documents scientifiques de niveau recherche, publiés ou non, émanant des établissements d'enseignement et de recherche français ou étrangers, des laboratoires publics ou privés.



Distributed under a Creative Commons Attribution 4.0 International License

Phase control of transmission and reflection in a sample of duplicated two-level systems driven by a stationary control field

F. A. Hashmi^{1,2}, E. Brion¹ and M. A. Bouchene¹

¹*Laboratoire Collisions Agrégats Réactivité, FeRMI,*

Université Toulouse III and CNRS UMR 5589, Toulouse, France and

²*Department of Physics, Syed Babar Ali School of Science and Engineering,
Lahore University of Management Sciences (LUMS), Lahore*

In this article, we investigate the optical response of a duplicated two-level atomic medium submitted to a strong stationary control field and a weak co-propagating probe field, orthogonally polarized to each other. We show that both reflected and transmitted components of the probe may be absorbed and amplified. Moreover, for low optical depths, reflection and transmission factors are controlled by the relative phase between control and probe fields, which makes the configuration we present here promising for the development of optical devices, such as phase-controlled switches.

I. INTRODUCTION

The control and manipulation of light pulses has long been a key challenge with many applications in, e.g., telecommunications and, more recently, quantum technologies. To achieve this goal one may try and shape the optical response of the propagation medium – absorption and /or dispersion – through combining non-linear effects and quantum interferences. Electromagnetic induced transparency (EIT) [1], refraction index enhancement [2], slow, stored and fast light [3] are examples of applications of such an approach. Meta-materials like negative-index samples [4] or photonics crystals [5] are based on different strategies. In the latter, the propagation of light is modified by the existence of photonic band gaps due to periodic spatial variations of the optical index, in the same way as periodic atomic lattices affect the conductivity of electrons in semiconductors. Such crystals are usually obtained by stacking dielectric slabs of different indices periodically. The optical features of the structures thus obtained are determined once and for all. Another more versatile way to obtain a photonic crystal is provided by Electromagnetically Induced Gratings (EIG). In this case, the periodic modulation of the medium optical response results from the application of a standing-wave driving field, which gives rise to new original phenomena. For instance, the standing-wave configuration was recognized years ago to be very promising to achieve spatial localization [6]. Moreover, exciting a lambda system in EIT configuration with a stationary control field one obtains a periodic modulation of the atomic absorption with sharp peaks which allows for the creation of stationary pulses of light [7] as well as the optical control of photonic band gaps [8]. Many groups also use this configuration to control the group velocity [9], induce Raman-gratings [10], phase-gratings [11], or implement phase-gates and optical switching [12].

In the present work, we focus on an atomic medium with the so-called duplicated two-level system (DTLS) configuration, often used to study electron spin coherence effects [13]. When excited by a strong control and a weak probe beams, polarized orthogonally to each other, DTLS exhibits efficient quantum interferences between absorption and stimulated emission paths. We pointed out the great potentialities of DTLS media for controlling the propagation of the probe field in previous works. We experimentally demonstrated the coherent control of the medium gain in the femtosecond regime [14]. We also theoretically predicted the existence of Zeeman-coherent-oscillation-assisted slowing of the probe in a non-collinear configuration [15] and phase control of the effective susceptibility in a collinear configuration [16]. Other authors proposed to take advantage of DTLS media to control optical bistability [17], group velocity [18], and implement quantum memory or optical switching [19]. It was also suggested to use orthogonal spatial configuration for the control field to generate spatial diffraction within the multiphoton resonance condition [20] or beyond [21]. The phase control of spatial interference of resonance fluorescence [22], transmission and reflection factors in a dielectric slab [23], and the possibility of spatial localization of atoms [24] are among promising related results.

In the present article, we consider a DTLS medium submitted to collinear control and probe fields. The control field, however, is now a standing-wave which induces an EIG in Zeeman coherences. The overlap between the control and probe beams ensures efficient interaction and energy exchange between the field components along the sample. We study the influence of interaction parameters – control field intensity, detuning, optical depth and phase shift between the control and the probe – on reflected and transmitted probe light intensity and phase. By contrast with transverse gratings which only diffract a weak part of the probe field, the optical depth of DTLS medium leads to significant reflection and transmission coefficients which can be even larger than one. This spatial configuration moreover enables a phase control of probe reflection and transmission in certain conditions we identify.

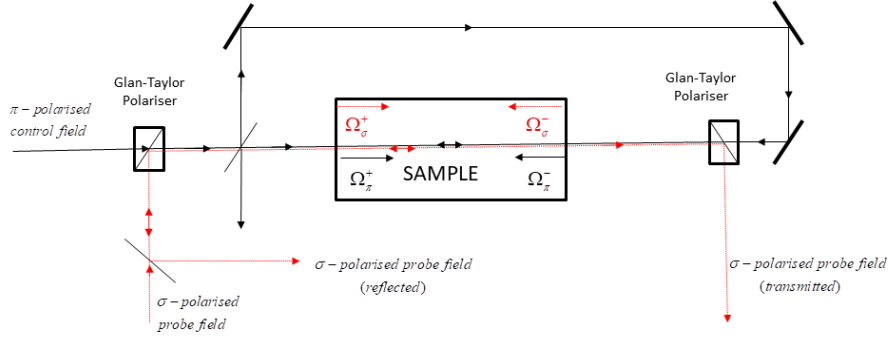


Figure 1. Experimental configuration (proposal). The control field is split into two parts that give the forward and backward components (Rabi envelopes Ω_π^\pm , respectively). The probe field is sent at the entrance of the sample in the forward direction (Rabi envelope Ω_σ^+) and the backward component (Rabi envelope Ω_σ^-) is generated from the end part of the sample.

II. THEORETICAL MODEL

A. The system

We consider the experimental configuration depicted in Fig. 1. An atomic sample of length L is submitted to two fields of same frequency ω , propagating along the y axis with orthogonal polarizations. The first – so-called control – field is π -polarized and split into two parts: one part penetrates the sample from the left side (henceforth designated as the entrance), and propagates in the direction of increasing y 's, while the other part is seeded back into the sample from the other side (henceforth designated as the exit), and propagates in the direction of decreasing y 's. The total control electric field expresses as

$$\mathbf{E}_\pi(y, t) = \mathbf{e}_z [\varepsilon_\pi^+(y) e^{iky} + \varepsilon_\pi^-(y) e^{-iky}] e^{-i\omega t} + \text{c.c.} \quad (1)$$

For sake of simplicity, we assume that the amplitude $\varepsilon_\pi^+(y=0)$ is real. The second – so-called probe – field is σ -polarized propagates in the direction of increasing y 's and penetrates the sample through the entrance. Its electric field is given by

$$\mathbf{E}_\sigma(y, t) = \mathbf{e}_x [\varepsilon_\sigma^+(y) e^{iky} + \varepsilon_\sigma^-(y) e^{-iky}] e^{-i\varphi} e^{-i\omega t} + \text{c.c.} \quad (2)$$

In this expression, φ is defined as the phase shift between the probe and control fields. Note that even if the injected probe field propagates in the forward direction, a backward component $\varepsilon_\sigma^-(y)$ builds up because the atomic sample radiates in both directions. Moreover, the boundary conditions for the probe at the exit and entrance write $\varepsilon_\sigma^-(y=L) = 0$ and $\varepsilon_\sigma^+(y=0) = E_0$, where E_0 is real.

We assume that the fields essentially couple to a $F = 1/2 \rightarrow F = 1/2$ atomic line of the medium (e.g. ${}^2S_{1/2}F = 1/2 \rightarrow {}^2P_{1/2}F = 1/2$ transition of ${}^6\text{Li}$ at 671 nm) described by a duplicated two-level system (Fig. 2). The π -polarized control field \mathbf{E}_π (resp. σ polarized probe field \mathbf{E}_σ) couples to the $\Delta m_F = 0$ (resp. $\Delta m_F = \pm 1$) paths. In the following, we determine the reflection and transmission coefficients of the medium for a weak probe in the presence of a much stronger control field.

B. Atomic polarization

In the interaction picture, the density matrix ρ of an atom in the medium obeys the master equation $i\hbar\partial_t\rho = [H, \rho] + \text{relaxations}$ where H is the Hamiltonian in the rotating wave approximation

$$H = \hbar \begin{pmatrix} 0 & 0 & -\Omega_\pi^* & -\Omega_\sigma^* e^{i\varphi} \\ 0 & 0 & -\Omega_\sigma^* e^{i\varphi} & \Omega_\pi^* \\ -\Omega_\pi & -\Omega_\sigma e^{-i\varphi} & \Delta_0 & 0 \\ -\Omega_\sigma e^{-i\varphi} & \Omega_\pi & 0 & \Delta_0 \end{pmatrix}$$

Here $\Omega_{j=\pi,\sigma} = \frac{d\varepsilon_j}{\hbar}$ denote the Rabi frequencies for the control and probe fields, with $d = \langle m_F = 1/2 | \mathbf{D} \cdot \mathbf{e}_z | m_F = 1/2 \rangle$ the z -component of the dipole moment of the transition ($F = 1/2, m_F = 1/2 \rightarrow F = 1/2, m_F = 1/2$), $\Delta_0 = \omega_0 - \omega$ is

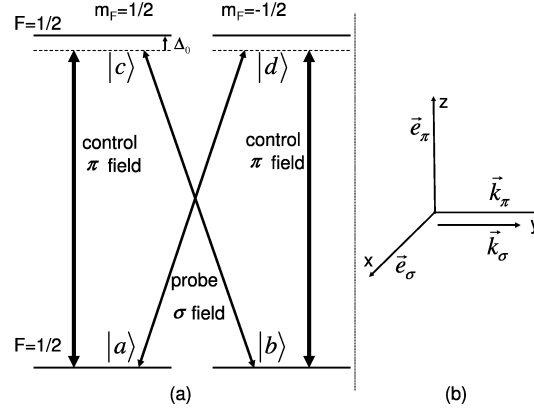


Figure 2. (a) The duplicated two-level system (DTLS) and (b) field configurations.

the detuning of the fields with respect to the DTLS natural frequency, ω_0 , while $\varepsilon_{j=\pi,\sigma}(y) = \varepsilon_j^+(y) + \varepsilon_j^-(y)e^{-2iky}$ are the envelopes of the control and probe fields, respectively. The populations ρ_{cc} and ρ_{dd} relax with the rate Γ , the coherences ρ_{ac} , ρ_{ad} , ρ_{bc} and ρ_{bd} with the rate Γ_d and the excited Zeeman coherence with the rate Γ_{ze} . In the absence of non-radiative homogeneous dephasing processes, (Γ_{ze}, Γ_d) reduce to $(\Gamma, \frac{\Gamma}{2})$. The modification of the probe field is determined by the behaviour of the coherence $\rho_\sigma = \rho_{cb} + \rho_{da}$ which radiates the σ -polarized light and whose evolution is ruled by the equation [14–16]

$$\partial_t \rho_\sigma = i\Omega_\pi (\rho_Z - \rho_Z^*) + i\Omega_\sigma e^{-i\varphi} (n_g - n_e) - (i\Delta_\pi + \Gamma_d) \rho_\sigma$$

where $\rho_Z = \rho_{ab} + \rho_{cd}$. The coherence ρ_σ therefore builds up through two competing phenomena, *i.e.* the diffraction of the pump by the Zeeman coherences (first term) and the absorption of the probe by the population (second term). In the stationary regime, the excited state coherence is destroyed by relaxations, $\rho_{cd} = 0$, and only the ground state Zeeman coherence ρ_{ab} contributes to ρ_σ . In the stationary regime, one finds $\rho_\sigma = 2\rho_{da} = 2\rho_{cb} = \left(\frac{\Omega_\sigma e^{-i\varphi}}{\Omega_\pi}\right)^* \rho_\pi$ with

$$\rho_\pi = \frac{(\Omega_\pi^2 + \Omega_\sigma^2 e^{-2i\varphi}) (i\Gamma_d + \Delta_0) \Omega_\pi^*}{4\Gamma_d \Gamma^{-1} |\Omega_\pi^2 + \Omega_\sigma^2 e^{-2i\varphi}|^2 + (|\Omega_\pi|^2 + |\Omega_\sigma|^2) (\Gamma_d^2 + \Delta_0^2)} \quad (3)$$

$$\rho_\sigma = \frac{(\Omega_\pi^2 + \Omega_\sigma^2 e^{-2i\varphi}) (i\Gamma_d + \Delta_0) \Omega_\sigma^* e^{i\varphi}}{4\Gamma_d \Gamma^{-1} |\Omega_\pi^2 + \Omega_\sigma^2 e^{-2i\varphi}|^2 + (|\Omega_\pi|^2 + |\Omega_\sigma|^2) (\Gamma_d^2 + \Delta_0^2)} \quad (4)$$

Throughout this work, we will assume that, along the sample, the control is much more intense than the probe, *i.e.*

$$|\Omega_\pi(y)| \gg |\Omega_\sigma(y)| \quad (5)$$

therefore, from Eqs.(3,4), we get

$$\rho_\pi = \frac{i\Gamma_d + \Delta_0}{4\Gamma_d \Gamma^{-1} |\Omega_\pi|^2 + \Gamma_d^2 + \Delta_0^2} \Omega_\pi \quad (6)$$

$$\rho_\sigma = \frac{i\Gamma_d + \Delta_0}{4\Gamma_d \Gamma^{-1} |\Omega_\pi|^2 + \Gamma_d^2 + \Delta_0^2} \frac{\Omega_\pi^2}{|\Omega_\pi|^2} \Omega_\sigma^* e^{i\varphi} \quad (7)$$

We now define $\alpha_0 = N d^2 \omega_0 / 2c \hbar \varepsilon_0 \Gamma_d$ the field absorption coefficient at resonance, where N denotes the number of atoms per unit volume in the medium, and we introduce χ_{lin} and χ_{sat} , the linear and saturated susceptibilities respectively, and χ_{eff} – whose signification will be given later,

$$\chi_{lin} = \frac{2\alpha_0 \Gamma_d / k}{-i\Gamma_d + \Delta_0} \quad (8)$$

$$\chi_{sat} = \chi_{lin} S \quad (9)$$

$$\chi_{eff} = \chi_{sat} e^{2i\varphi} \quad (10)$$

with the saturation parameter $S(y)$ defined as

$$S(y) = \frac{1}{1 + F_0 |\Omega_\pi(y)|^2} \quad (11)$$

and

$$F_0 = \frac{4\Gamma_d \Gamma^{-1}}{\Gamma_d^2 + \Delta_0^2} \quad (12)$$

Using Eqs.(6-12), we finally get

$$\rho_\pi = \left(\frac{k}{2\alpha_0 \Gamma_d} \right) \chi_{sat} \Omega_\pi \quad (13)$$

$$\rho_\sigma = \left(\frac{k}{2\alpha_0 \Gamma_d} \right) \chi_{eff} \frac{\Omega_\pi^2}{|\Omega_\pi|^2} \Omega_\sigma^* e^{-i\varphi} \quad (14)$$

C. Propagation equations

The control and probe fields obey the following one-dimensional Maxwell propagation equations

$$\begin{aligned} \frac{\partial^2}{\partial y^2} (\Omega_\pi e^{iky}) + k^2 (\Omega_\pi e^{iky}) &= -2k\alpha_0 \Gamma_d (\rho_\pi e^{iky}) \\ \frac{\partial^2}{\partial y^2} (\Omega_\sigma e^{iky} e^{-i\varphi}) + k^2 (\Omega_\sigma e^{iky} e^{-i\varphi}) &= -2k\alpha_0 \Gamma_d (\rho_\sigma e^{iky}) \end{aligned}$$

Using Eqs.(1,2), we explicitly decompose the Rabi frequencies into their forward and backward contributions

$$\Omega_{j=\pi,\sigma}(y) = \Omega_j^+(y) + \Omega_j^-(y) e^{-2iky} \quad (15)$$

with $\Omega_{j=\pi,\sigma}^\pm = \frac{d\varepsilon_j^\pm}{\hbar}$, and we define the associated phases φ_j^\pm by the relation $\Omega_j^\pm = |\Omega_j^\pm| e^{-i\varphi_j^\pm}$. We also formally expand the coherences $\rho_{j=\pi,\sigma}$ as

$$\rho_j(y) = \sum_{n=-\infty}^{+\infty} \rho_j^{(n)}(y) e^{2in ky} \quad (16)$$

When the conditions $\left| \frac{\partial^2}{\partial y^2} \Omega_j^\pm \right| \ll k \left| \frac{\partial}{\partial y} \Omega_j^\pm \right| \ll k^2 |\Omega_j^\pm|$ are met, the slow envelope approximation can be performed. The envelopes $\rho_j^{(n)}(y)$ are then slowly varying at the wavelength scale. Retaining only the relevant terms $\rho_j^{(n)}(y)$ which satisfy the phase matching condition, one finally gets from Eqs.(14-16)

$$\frac{\partial \Omega_\pi^+}{\partial y} = i\alpha_0 \Gamma_d \rho_\pi^{(0)} \quad (17)$$

$$\frac{\partial \Omega_\pi^-}{\partial y} = -i\alpha_0 \Gamma_d \rho_\pi^{(-1)} \quad (18)$$

$$\frac{\partial \Omega_\sigma^+}{\partial y} = i\alpha_0 \Gamma_d e^{i\varphi} \rho_\sigma^{(0)} \quad (19)$$

$$\frac{\partial \Omega_\sigma^-}{\partial y} = -i\alpha_0 \Gamma_d e^{i\varphi} \rho_\sigma^{(-1)} \quad (20)$$

In the next section, we recall important results on the simpler specific case when control and probe beams are both forward-propagating. Then, in Sec. IV, we shall address the more complex configuration involving a stationary control field and investigate in detail the observed phase-controlled probe reflection and transmission through analysing the behaviour of associated coefficients $R = \left| \frac{\Omega_\sigma^-(y=L)}{\Omega_\pi^+(y=0)} \right|^2$ and $T = \left| \frac{\Omega_\pi^+(y=L)}{\Omega_\pi^+(y=0)} \right|^2$.

III. SITUATION WITH NO BACKWARD CONTROL FIELD

We first address the case of forward-propagating fields inside the medium, *i.e.* $\varepsilon_j^-(y) = 0$, $\Omega_j = \Omega_j^+$ and $\rho_j = \rho_j^{(0)}$ for $j = \pi, \sigma$. This situation has been studied in detail in [16], we shall therefore only briefly summarize the main effects here.

Using the relation $\frac{\Omega_\pi^2}{|\Omega_\pi|^2} \Omega_\sigma^* = e^{2i\Delta\varphi_{\sigma\pi}^+} \Omega_\sigma^+$ with $\Delta\varphi_{\sigma\pi}^+ = \varphi_\sigma^+ - \varphi_\pi^+$, Eqs.(13, 14, 17-20) lead to

$$\frac{\partial \Omega_\pi^+}{\partial y} = i \frac{k}{2} \chi_{sat} \Omega_\pi^+ \quad (21)$$

$$\frac{\partial (\Omega_\sigma^+ e^{-i\varphi})}{\partial y} = i \frac{k}{2} \chi_{eff} e^{2i\Delta\varphi_{\sigma\pi}^+} (\Omega_\sigma^+ e^{-i\varphi}) \quad (22)$$

Provided that the dephasing between the control and probe fields, denoted by $\Delta\varphi_{\sigma\pi}^+$, does not substantially grow along propagation, χ_{eff} is seen to play the role of an effective susceptibility for the probe in Eq.(22). From Eqs.(21,22), one derives the propagation equation

$$\frac{\partial \Delta\varphi_{\sigma\pi}^+}{\partial y} = k \sin(\Delta\varphi_{\sigma\pi}^+ - \varphi) [\chi'_{sat} \sin(\Delta\varphi_{\sigma\pi}^+ - \varphi) - \chi''_{sat} \cos(\Delta\varphi_{\sigma\pi}^+ - \varphi)] \quad (23)$$

where χ'_{sat} and χ''_{sat} denote the real and imaginary parts of the saturated susceptibility, respectively. We introduce the phase of the linear susceptibility, φ_L , defined by $\chi_{lin} = |\chi_{lin}| e^{i\varphi_L}$, which verifies

$$\tan \varphi_L = \frac{\Gamma_d}{\Delta_0} \quad (24)$$

The integration Eq.(23) leads to $\tan \Delta\varphi_{\sigma\pi}^+ = \frac{\tan \varphi_L}{\left(\frac{\tan \varphi_L}{\tan \varphi} + 1\right) e^{-2\alpha_0 y \sin^2 \varphi_L} - 1}$. When $|\Omega_\pi(y=0)| \ll \sqrt{\Gamma_d \Gamma}$ and $\alpha_0 L \sin^2 \varphi_L \ll 1$, then $|\Omega_\pi^+(y)| \approx |\Omega_\pi^+(y=0)|$, $S \approx 1$ and $\Delta\varphi_{\sigma\pi}^+ \approx 0$, see [16]. The sample therefore becomes a linear medium for the probe field whose susceptibility, χ_{eff} , is related to the true linear susceptibility through $\chi_{eff} = \chi_{lin} e^{2i\varphi}$. The latter relation proves the existence of the phase control of the linear response of the medium, whose physical interpretation was described in [16]. It results from interference effects between the quantum paths which contribute to the coherence ρ_σ responsible for the σ -polarized radiated field.

If the control field intensity is increased, saturation effects occur and the validity condition of parametric approximation is less restrictive. From Eq.(21), one gets

$$\frac{\partial |\Omega_\pi^+|}{\partial y} = -\alpha_0 S \sin^2 \varphi_L |\Omega_\pi^+|$$

and provided that $\alpha_0 L S (y=0) \sin^2 \varphi_L \ll 1$, control field intensity remains unaffected along propagation. If the optical depth is increased so that the inequality $\alpha_0 L S (y=0) \sin^2 \varphi_L \ll 1$ no longer holds, the modification of the control field cannot be neglected and additional dephasing has to be taken into account in the propagation equation of the probe. New features appear and are detailed in [16].

IV. SITUATION OF A STATIONARY CONTROL FIELD

In this section, we investigate the effects which appear when the intensity of the control field is not uniform but spatially modulated because of the backward component. In this situation, the probe field experiences both reflexion and transmission. The impact of the modification of the optical response of the sample and the eventuality of phase control can be evaluated by calculating the transmission and reflection coefficients for the probe field.

A. Propagation equations in the slow envelope approximation

In the slow envelope approximation, the set of Eqs.(17-20) can be rewritten by extracting an analytical expression for the components $\rho_j^{(0)}(y)$ and $\rho_j^{(-1)}(y)$.

We introduce the parameter $r(y)$ and phase φ_r defined by $\Omega_\pi^-(y) = r(y) \Omega_\pi^+(y)$ and $r = |r| e^{-i\varphi_r}$, so that $\varphi_r = \varphi_\pi^- - \varphi_\pi^+$. When the control field is unaffected by the propagation, $r(y)$ is constant. Note that, for Eq.(5) to hold,

the control field should not vanish anywhere, including the spatial nodes, therefore r should be different from 1. From Eqs.(13,14,16), we see that the analytical expressions of $\rho_j^{(0)}(y)$ and $\rho_j^{(-1)}(y)$ can be evaluated as soon as the series expansion of the saturation parameter $S(y)$ and $\frac{1}{|\Omega_\pi(y)|^2}$ are determined. The saturation parameter S given by Eq.(11) may be expressed as

$$S(y) = \frac{b(y)}{1 + a(y) \cos [2ky + \varphi_r(y)]} \quad (25)$$

with $a(y) = \frac{2F_0 |\Omega_\pi^+(y)|^2 |r(y)|}{1 + F_0 |\Omega_\pi^+(y)|^2 (1 + |r(y)|^2)}$ and $b(y) = \frac{1}{1 + F_0 |\Omega_\pi^+(y)|^2 (1 + |r(y)|^2)}$. It can also be formally expanded as

$$S(y) = \sum_{n=-\infty}^{+\infty} c_n(y) e^{2inky} \quad (26)$$

where the c_n coefficients are slowly varying at the spatial wavelength scale $2\pi/k$ and can be approximated as $c_n(y) \approx \frac{k}{\pi} \int_y^{y+\pi/k} S(y') e^{-2inky'} dy'$. For $n \geq 0$, using Eq.(25) and [25], we get $c_n(y) \approx c_0 \eta^n e^{in\varphi_r(y)}$, with $c_0 = \frac{b(y)}{\sqrt{1-a^2(y)}}$ and $\eta = \frac{\sqrt{1-a^2(y)}-1}{a(y)}$. Moreover, for $n \leq 0$, the reality of parameter S implies that $c_n = c_{-n}^*$.

On the other hand, using Eq.(15), one may put the parameter $\frac{1}{|\Omega_\pi(y)|^2}$ under the form

$$\frac{1}{|\Omega_\pi(y)|^2} = \frac{b'(y)}{1 + a'(y) \cos [2ky + \varphi_r(y)]} \quad (27)$$

with $a'(y) = \frac{2|r(y)|}{|\Omega_\pi^+(y)|^2 (1 + |r(y)|^2)}$ and $b'(y) = \frac{1}{|\Omega_\pi^+(y)|^2 (1 + |r(y)|^2)}$. It can also be formally expanded as $\frac{1}{|\Omega_\pi(y)|^2} = \sum_{n=-\infty}^{+\infty} c'_n(y) e^{2inky}$ where the c'_n coefficients are slowly varying at the wavelength scale and can be expressed as $c'_n(y) \approx \frac{k}{\pi} \int_y^{y+\pi/k} \frac{1}{|\Omega_\pi(y')|^2} e^{-2inky'} dy'$. Using [25], we get $c'_{n \geq 0}(y) \approx c'_0 \eta'^n e^{in\varphi_r(y)}$ with $c'_0 = \frac{b'(y)}{\sqrt{1-a'^2(y)}}$ and $\eta' = \frac{\sqrt{1-a'^2(y)}-1}{a'(y)}$. Moreover, the reality of $\frac{1}{|\Omega_\pi|^2}$ implies that $c'_{n \leq 0} = (c'_{-n})^*$.

Using Eqs.(13,14,16,25,26,27), we can finally express the components of the coherences which appear in the propagation equations for the control fields

$$\rho_\pi^{(0)}(y) = \frac{i}{\Gamma_d} [\bar{c}_0(y) \Omega_\pi^+(y) + \bar{c}_1(y) \Omega_\pi^-(y)] \quad (28)$$

$$\rho_\pi^{(-1)}(y) = \frac{i}{\Gamma_d} [\bar{c}_{-1}(y) \Omega_\pi^+(y) + \bar{c}_0(y) \Omega_\pi^-(y)] \quad (29)$$

with $\bar{c}_i(y) = \left(\frac{\Gamma_d}{\Gamma_d + i\Delta_0} \right) c_i(y)$, and in the propagation equations for the probe fields

$$\rho_\sigma^{(0)}(y) = \frac{i}{\Gamma_d} e^{i\varphi} [c_+(y) \Omega_\sigma^{+*}(y) + c_{+-}(y) \Omega_\sigma^{-*}(y)] \quad (30)$$

$$\rho_\sigma^{(-1)}(y) = \frac{i}{\Gamma_d} e^{i\varphi} [c_{+-}(y) \Omega_\sigma^{+*}(y) + c_-(y) \Omega_\sigma^{-*}(y)] \quad (31)$$

with

$$c_+ = \beta \left[1 + 2\gamma |r| + \delta |r|^2 \right] \quad (32)$$

$$c_{+-} = \beta r \left[2 + \frac{\gamma}{|r|} + \gamma |r| \right]$$

$$c_- = \beta r^2 \left[1 + \frac{2\gamma}{|r|} + \frac{\delta}{|r|^2} \right]$$

and

$$\beta = \frac{c_0 e^{-2i\varphi_\pi^+}}{(1 - \eta\eta') |1 - |r|^2|} \left(\frac{\Gamma_d}{\Gamma_d + i\Delta_0} \right) \quad (33)$$

$$\gamma = \eta + \eta' \quad (34)$$

$$\delta = \eta^2 + (\eta')^2 + \eta\eta' - (\eta\eta')^2 \quad (35)$$

Injecting Eqs.(28-31) into Eqs.(17,18) and Eqs.(19,20), we get

$$\frac{\partial \Omega_{\pi}^{+}}{\partial (y/L)}(y) = -\alpha_0 L [\bar{c}_0(y) \Omega_{\pi}^{+}(y) + \bar{c}_1(y) \Omega_{\pi}^{-}(y)] \quad (36)$$

$$\frac{\partial \Omega_{\pi}^{-}}{\partial (y/L)}(y) = \alpha_0 L [\bar{c}_{-1}(y) \Omega_{\pi}^{+}(y) + \bar{c}_0(y) \Omega_{\pi}^{-}(y)] \quad (37)$$

and

$$\frac{\partial \Omega_{\sigma}^{+}}{\partial (y/L)}(y) = -\alpha_0 L e^{2i\varphi} [c_{+}(y) \Omega_{\sigma}^{+*}(y) + c_{+-}(y) \Omega_{\sigma}^{-*}(y)] \quad (38)$$

$$\frac{\partial \Omega_{\sigma}^{-}}{\partial (y/L)}(y) = \alpha_0 L e^{2i\varphi} [c_{+-}(y) \Omega_{\sigma}^{+*}(y) + c_{-}(y) \Omega_{\sigma}^{-*}(y)] \quad (39)$$

The forward and backward components of both the probe and control fields are now coupled through the coefficients $(\bar{c}_{-1}, \bar{c}_1)$ for the control and c_{+-} coefficient for the probe. In particular, Eqs.(38,39) clearly show that the probe field propagation may be controlled by the phase. This property is further investigated in Sec. V, through numerically solving the above coupled equations.

B. Limit of small optical depths

The probe field propagation depends on the control field intensity and the optical depth. For small optical depths, *i.e.* $|\alpha_0 L \bar{c}_{j=0,\pm 1}| \ll 1$, the control field is weakly affected by propagation and the envelopes can be considered uniform, *i.e.* $\Omega_{\pi}^{+}(y) \approx \Omega_{\pi}^{+}(0)$, $\Omega_{\pi}^{-}(y) \approx \Omega_{\pi}^{-}(L)$ and $\varphi_{\pi}^{\pm} \approx 0$. The coefficients c_{+}, c_{-}, c_{+-} are thus constant along the sample and the phases φ_{π}^{+} and φ_{π}^{-} are neglected. The system of Eqs.(38,39) turns into a set of differential equations with constant coefficients. Moreover, for optical depths such as $|\alpha_0 L c_{j=+,-,+-}| \ll 1$, one may retain the most significant terms in the integration of the system Eqs.(38,39) which leads to

$$\begin{aligned} \Omega_{\sigma}^{+}(y) - \Omega_{\sigma}^{+}(0) &\approx -\alpha_0 y e^{2i\varphi} [c_{+} \Omega_{\sigma}^{+*}(0) + c_{+-} \Omega_{\sigma}^{-*}(0)] \\ \Omega_{\sigma}^{-}(y) - \Omega_{\sigma}^{-}(L) &\approx \alpha_0 (y - L) e^{2i\varphi} [c_{+-} \Omega_{\sigma}^{+*}(L) + c_{-} \Omega_{\sigma}^{-*}(L)] \end{aligned}$$

Taking into account the boundary condition $\{\Omega_{\sigma}^{-}(L) = 0; \Omega_{\sigma}^{+*}(0) = \Omega_{\sigma}^{+}(0)\}$, one readily obtains

$$\Omega_{\sigma}^{+}(y) \approx \Omega_{\sigma}^{+}(0) [1 - \alpha_0 y e^{2i\varphi} c_{+}] \quad (40)$$

$$\Omega_{\sigma}^{-}(y) \approx \Omega_{\sigma}^{-}(0) \alpha_0 (y - L) e^{2i\varphi} [c_{+-} - \alpha_0 (y - L) e^{-2i\varphi} c_{+-} c_{+}^*] \quad (41)$$

From Eqs.(32,33-37), we get $\arg[c_{+}(0)] = \varphi_L - \pi/2$, where φ_L is defined in Eq.(24). Transmission and reflection coefficients can then be approximated as

$$T \approx 1 - 2\alpha_0 L |c_{+}| \sin(2\varphi + \varphi_L) \quad (42)$$

$$R \approx |\alpha_0 L c_{+-}|^2 [1 - 2\alpha_0 L |c_{+}| \sin(2\varphi + \varphi_L)] \quad (43)$$

These expressions show the existence of phase-controlled reflection and transmission in the limit of small optical depths. The coefficients can be modified by adjusting a versatile and fine tuning experimental parameter, φ , the additional shift φ_L being determined by the detuning Δ_0 . For $0 \leq 2\varphi + \varphi_L \leq \pi$, the transmission factor T is less or equal to 1, while it becomes larger than 1 for $\pi \leq 2\varphi + \varphi_L \leq 2\pi$. This is in agreement with the absorptive or amplificative nature of the sample as described by its effective linear susceptibility, given by Eq.(10). The reflection factor is associated with the backward component of the control field that is generated through the coupling with the forward part of the probe. Thus, the reflection factor depends on the second (or higher) power of the optical depth and is small with respect to the transmission factor. As for the transmission factor, however, the contrast is linear with the optical depth and can be varied by modifying the intensities of the control field components.

V. RESULTS AND DISCUSSION

In this section, we present both the numerical results obtained through the numerical simulation of Eqs.(36-39) and analytical approximation, Eqs.(42,43), and discuss their physical interpretation.

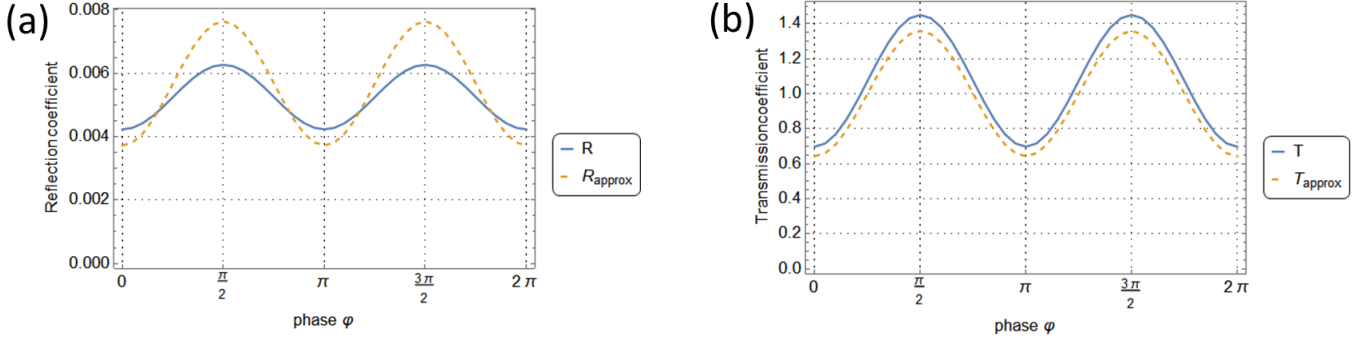


Figure 3. (a) Reflection and (b) Transmission factors as functions of the relative phase φ at resonance ($\Delta_0 = 0$) for a probe field propagating in an optically thin sample (optical depth $\alpha_0 L = 0.3$) driven by a control field with Rabi amplitudes $\Omega_\pi^+(0)/\Gamma_d = 0.4$ and $\Omega_\pi^-(L)/\Gamma_d = 0.16$. Blue solid (orange dashed) line plots are obtained through numerical simulation (analytic approximation).

In Fig.3 are plotted the variations of the (a) reflection, R , and (b) transmission, T , coefficients as functions of the relative phase φ , for resonant probe and control fields ($\Delta_0 = 0$) and small optical depth $\alpha_0 L = 0.3$. Forward/backward control field Rabi frequencies at the entrance/exit of the sample are set to $\frac{\Omega_\pi^+(0)}{\Gamma_d} = 0.4$ and $\frac{\Omega_\pi^-(L)}{\Gamma_d} = 0.16$, respectively. The curves in solid and dashed lines correspond to numerical simulations and approximate analytical expressions, Eqs.(42,43), respectively. We observe that both R and T oscillate with a period of π as expected from the $e^{2i\varphi}$ dependence of the effective susceptibility, Eq.(10). As already pointed out in Subsec. IV B, T may be larger or smaller than 1, depending whether the sample is amplificative or absorptive. We note that T is much larger than R : the transmitted field indeed results from the interference of the incident and radiated probe fields, while, in contrast, the reflected field results from the backward radiated field only and is thus proportional to the small optical depth. Moreover, we observe discrepancies between the numerical simulations and the simple perturbative analytical model.

In Fig. 4 are plotted (a) the (normalized) backward and forward-propagating control field intensities $\left| \frac{\Omega_\pi^\pm(y)}{\Gamma_d} \right|^2$ and (b) phases φ_π^\pm , respectively, as functions of the (normalized) position y/L , for the set of parameters $\Delta_0 = 0$, $\alpha_0 L = 0.3$, $\Omega_\pi^+(0)/\Gamma_d = 0.4$, $\Omega_\pi^-(L)/\Gamma_d = 0.16$. Forward-propagating field intensity is attenuated by 37.5% along its propagation, from the input value 0.16 at the entrance to approximately 0.1 at the exit of the sample, while the backward-propagating control field intensity is reduced by 22%, from the input value 0.0256 at the exit to 0.02 at the entrance. The phases accumulated along propagation are small in all cases. This can be understood from Eqs.(36,37). At low optical depth, the dominant contribution due to the diagonal terms involves the \bar{c}_0 coefficient which is real at resonance. The control field components therefore experience pure absorption without dispersion, the accumulated phase is thus negligible. For the lowest-order solution of Eqs.(38,39), namely Eqs.(40,41), to hold, the condition $|\alpha_0 L c_j| \ll 1$ must be checked: we find the values 0.192, 0.005, 0.054 for $|\alpha_0 L c_{j=+, -, +}|$, respectively, which ensures the validity of the analytical model presented in Subsec. IV B, although the control field can be considered only roughly unaltered along propagation. This simple model captures the essential physical phenomena at work and clearly exhibits the accuracy of phase control of R and T .

Figs 5 and 6 correspond to the same situations as considered in Figs 3 and 4, though with a higher optical depth $\alpha_0 L = 0.6$. Both the reflection and transmission coefficients are significantly enhanced in Fig. 5 compared to Fig. 3: now, T oscillates between 0.48 and 2.17 – versus 0.7 and 1.45 for $\alpha_0 L = 0.3$ – and R between 0.017 and 0.043 – versus 0.0043 and 0.0063 for $\alpha_0 L = 0.3$. Here, although the parametric approximation is no longer valid, both R and T still depend on the phase and are substantially amplified. The fitting by the analytical model, Eqs.(42,43), is only qualitative for two reasons. First, as shown in Fig. 6, the increased optical depth leads to stronger absorption of the control field along propagation. The forward-, resp. backward-, propagating component intensity is indeed reduced by 60% (37% in the case of Fig. 4 with $\alpha_0 L = 0.3$), resp. 56% (22% in Fig. 4). The parametric approximation, $\Omega_\pi^+(y) \approx \Omega_\pi^+(0)$; $\Omega_\pi^-(y) \approx \Omega_\pi^-(L)$, is thus rough. Secondly, the coefficients $|\alpha_0 L c_{j=+, -, +}|$ are magnified approximately by a factor two with respect to the case where $\alpha_0 L = 0.3$ (e.g. $|\alpha_0 L c_j| \approx 0.41, 0.006, 0.09$ for $j = +, -, +$, respectively) making the low order perturbation solution less valid. Note that in this case the dispersive component of the optical response vanishes at resonance and therefore the phase remains essentially constant.

In Fig. 7 are plotted the (a) reflection and (b) transmission coefficients as functions of the relative phase φ , in the resonant case $\Delta_0 = 0$ (solid line) and the non-resonant case $\Delta_0/\Gamma_d = 2$ (dashed line), the other parameters being $\alpha_0 L = 0.3$ and $\Omega_\pi^+(0)/\Gamma_d = 0.4$, $\Omega_\pi^-(L)/\Gamma_d = 0.16$. When the detuning increases, the modulus of the effective susceptibility χ_{eff} , Eq.(10), decreases and so does the global coupling of the probe with the atomic medium. R and T

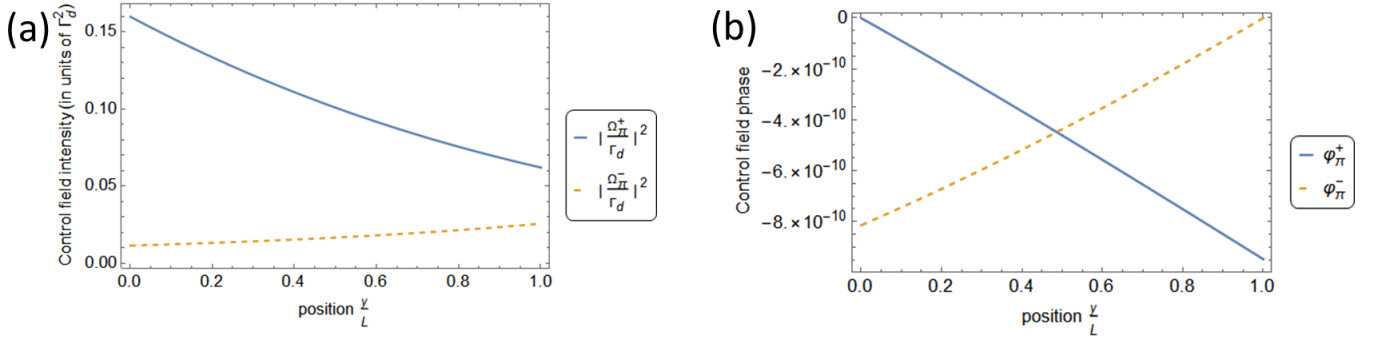


Figure 4. Control field (a) intensities $\left|\frac{\Omega_\pi^\pm}{\Gamma_d}\right|^2$ and (b) phases φ_π^\pm as functions of the (normalized) propagation distance y/L for $\Delta_0 = 0$, $\alpha_0 L = 0.3$, $\frac{\Omega_\pi^+(0)}{\Gamma_d} = 0.4$ and $\frac{\Omega_\pi^-(L)}{\Gamma_d} = 0.16$.

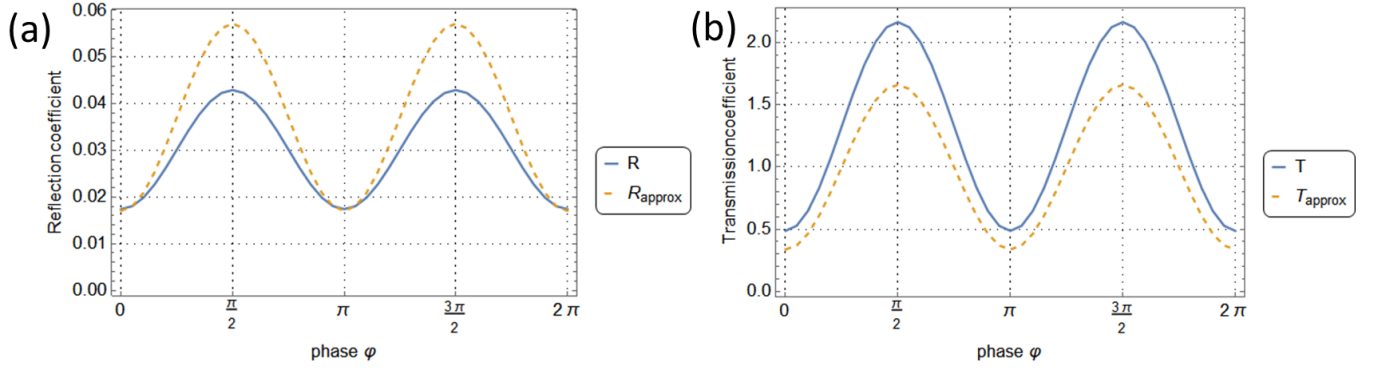


Figure 5. (a) Reflection and (b) Transmission factors as functions of the relative phase φ for $\Delta_0 = 0$, $\alpha_0 L = 0.6$, $\frac{\Omega_\pi^+(0)}{\Gamma_d} = 0.4$ and $\frac{\Omega_\pi^-(L)}{\Gamma_d} = 0.16$. Blue solid (resp. orange dashed) line plots are obtained through numerical simulation (resp. analytic approximation).

therefore tend to decrease, which is confirmed by the results of numerical simulation. An important feature, however, is the dephasing which appears on R and T plots when modifying the detuning. The expression of the phase shift predicted by the analytical model, Eqs.(42,43), is φ_L with $\tan \varphi_L = \Gamma_d/\Delta_0$. When $\Gamma_d/\Delta_0 = 0.5$, $\varphi_L \approx 0.15\pi$ which is very close to the value 0.16π obtained via numerical simulations.

In Fig. 8 are plotted the intensities of (a) the forward probe field, $|\Omega_\sigma^+(y)/\Omega_\sigma^+(0)|^2$, and (b) the backward probe field, $|\Omega_\sigma^-(y)/\Omega_\sigma^-(0)|^2$, as functions of the normalized coordinate y/L for three values of the relative phase $\varphi = 0, \pi/4, \pi/2$, and

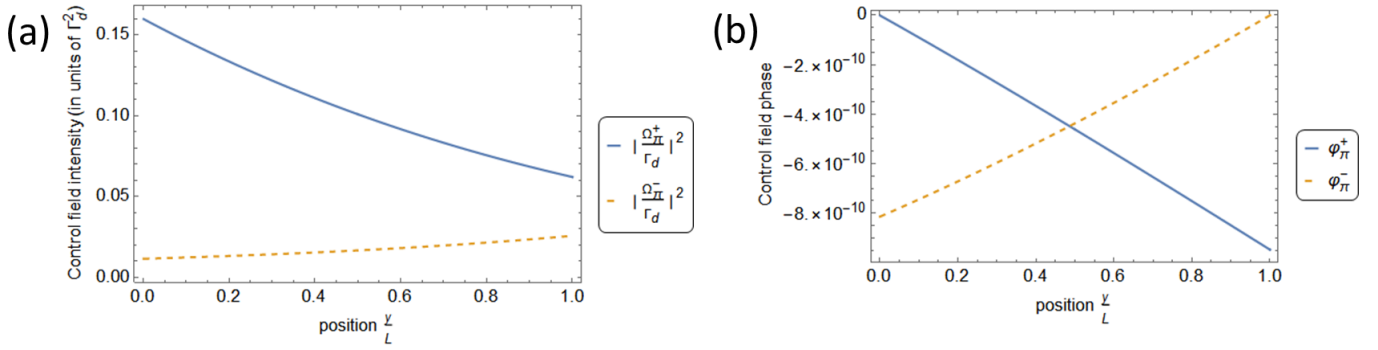


Figure 6. Control field (a) intensities $\left|\frac{\Omega_\pi^\pm}{\Gamma_d}\right|^2$ and (b) phases φ_π^\pm as functions of the (normalized) propagation distance y/L for $\Delta_0 = 0$, $\alpha_0 L = 0.6$, $\frac{\Omega_\pi^+(0)}{\Gamma_d} = 0.4$ and $\frac{\Omega_\pi^-(L)}{\Gamma_d} = 0.16$.

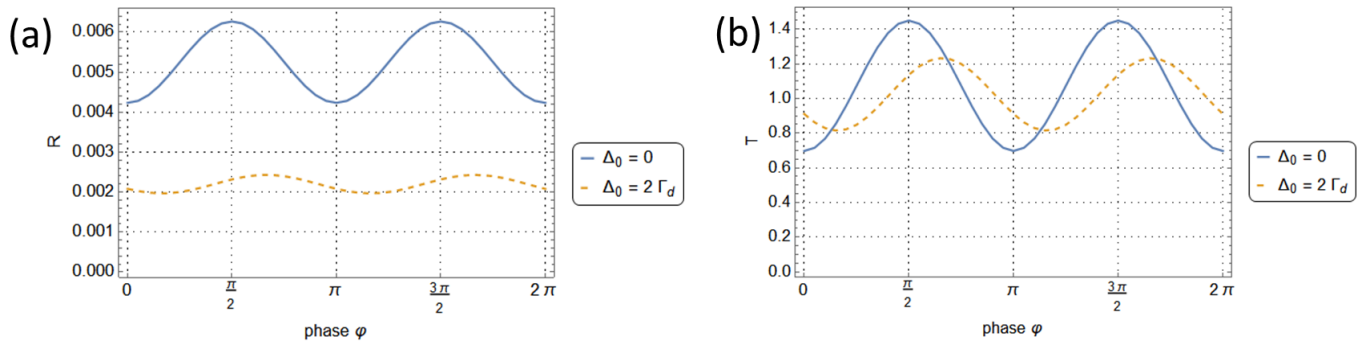


Figure 7. Effect of detuning. (a) Reflection and (b) Transmission factors plotted as functions of the relative phase φ for $\alpha_0 L = 0.3$, $\frac{\Omega_{\pi}^{+}(0)}{\Gamma_d} = 0.4$, $\frac{\Omega_{\pi}^{-}(L)}{\Gamma_d} = 0.16$ and $\Delta_0/\Gamma_d = 0$ (solid blue line), 2 (dashed orange line).

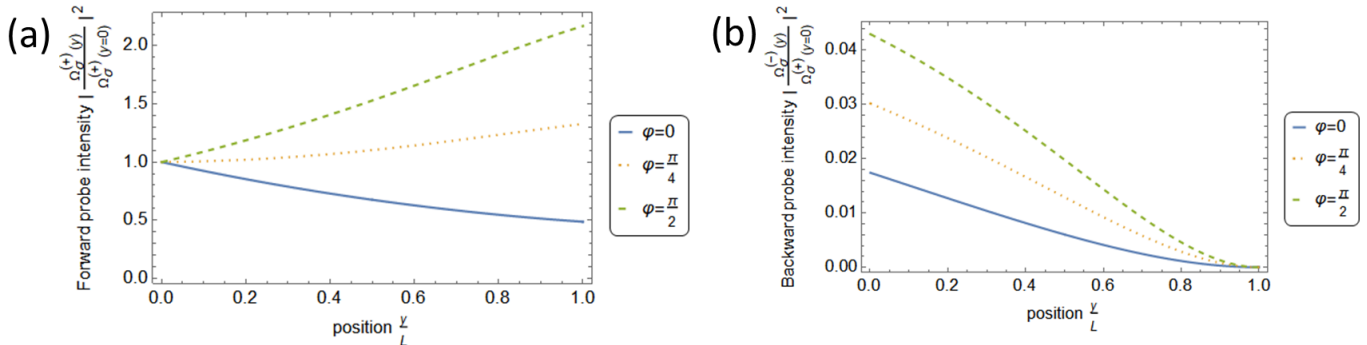


Figure 8. Probe field intensities (a) $\left| \frac{\Omega_{\sigma}^{+}(y)}{\Omega_{\sigma}^{+}(0)} \right|^2$ and (b) $\left| \frac{\Omega_{\sigma}^{-}(y)}{\Omega_{\sigma}^{-}(0)} \right|^2$ as functions of the (normalized) propagation distance y/L for $\varphi = 0$ (solid blue line), $\frac{\pi}{4}$ (dotted orange line), $\frac{\pi}{2}$ (dashed green line).

$\Delta_0 = 0$, $\Omega_{\pi}^{+}(0)/\Gamma_d = 0.4$, $\Omega_{\pi}^{-}(L)/\Gamma_d = 0.16$, $\alpha_0 L = 0.6$. In Figs. 9 (a,b) are plotted the corresponding accumulated phases $\varphi_{\sigma}^{\pm}(y)$. As shown by Fig. 8-a, $\varphi = 0$ leads to absorption of the forward component of the probe whereas $\varphi = \pi/2$ leads to its significant amplification. The case $\varphi = \pi/4$ corresponds to a small modification of the probe. This is in line with the results of the numerical simulations (Fig.5-a). We also notice that intensity depends quasi-linearly on the propagation distance which comforts the linear approximation performed in Eqs.(40,42). In Fig. 8-b, is represented the backward probe component which vanishes at $y = L$. The field is amplified from the exit to the entrance of the sample. Its intensity at the entrance depends significantly on the dephasing. On the other hand, the shape of the curves is almost parabolic around $y = L$. Indeed, when y is close to L , Eq.(41) yields $|\Omega_{\sigma}^{-}(y)|^2 \approx |\Omega_{\sigma}^{+}(0)|^2 |c_{+-}|^2 \alpha_0^2 (y - L)^2$.

The accumulated phase $\varphi_{\sigma}^{+}(y)$ and $\varphi_{\sigma}^{-}(y)$ are represented in Fig.9-a and b, respectively. The forward component exhibits a vanishing phase at the entrance and accumulates a significant value along propagation ($\varphi_{\sigma}^{+}(y = L) \approx 0.34$) for $\varphi = \pi/4$ whereas for $\varphi = 0$ and $\varphi = \pi/2$ the phase remains equal to zero. This effect can be explained from the simple analytical model introduced in Subsec. IV B which leads to Eq.(40). We then have $\varphi_{\sigma}^{+}(y) \approx -\alpha_0 y |c_{+}| \cos(2\varphi + \varphi_L)$. At resonance, $\varphi_L = \pi/2$ and thus $\varphi_{\sigma}^{+}(y) = 0$ for $\varphi = 0, \pi/2$ and $\varphi_{\sigma}^{+}(y) \approx \alpha_0 y |c_{+}|$ for $\varphi = \pi/4$. Using $|c_{+}(0)| = 0.683$, the analytical model predicts an accumulated phase $\varphi_{\sigma}^{+}(y = L) \approx 0.41$ to compare with the value 0.34 given by exact numerical simulations. The backward component has a different behavior. Indeed, due to the boundary condition $\Omega_{\sigma}^{-}(L) = 0$, the value of the phase φ_{σ}^{-} cannot be set either at the entrance ($y = 0$) or the exit ($y = L$) of the sample, only the propagation dynamics allows us to recover it. From Eq.(41), $\varphi_{\sigma}^{-}(y) \approx \pi - 2\varphi + \alpha_0 (y - L) |c_{+}| \cos(2\varphi + \varphi_L)$, which leads $\varphi_{\sigma}^{-}(L) \approx \pi, \pi/2, 0$ for $\varphi = 0, \pi/4$ and $\pi/2$ in agreement with the numerical values read on inset (b) of Fig. 9, *i.e.* 3.14, 1.35, 0, respectively.

VI. CONCLUSION

In this article, the dynamics of an ensemble of duplicated two-level systems driven by a strong stationary control field and subject to a weak probe field was studied in detail. In particular, the expressions of the probe reflection,

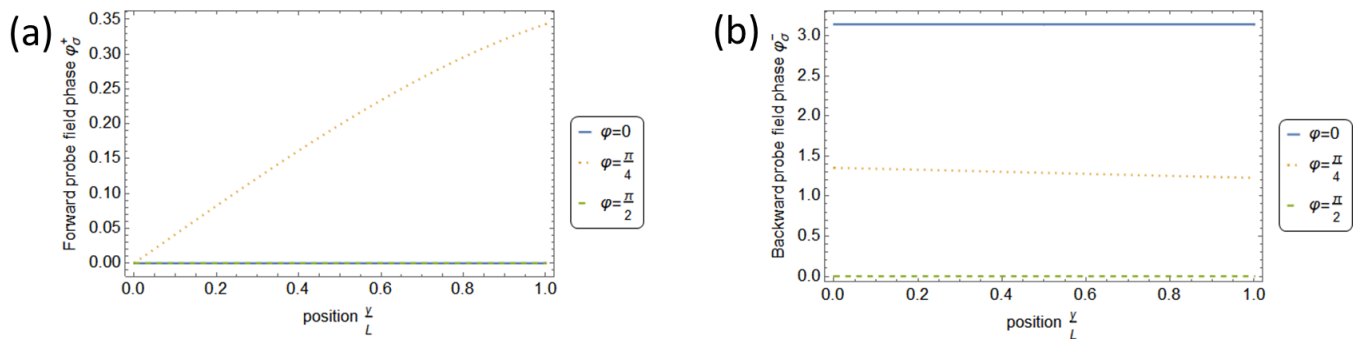


Figure 9. Accumulated phases (a) $\varphi_{\sigma}^{+}(y)$ of the forward-propagating probe field and (b) $\varphi_{\sigma}^{-}(y)$ of the backward-propagating probe field as functions of the (normalized) propagation distance y/L for $\varphi = 0$ (solid blue line), $\frac{\pi}{4}$ (dotted orange line), $\frac{\pi}{2}$ (dashed green line).

R , and transmission, T , factors were determined and their dependence on field parameters was investigated. Both amplification and absorption were shown to be achievable. Moreover, R and T depend on the relative phase between the fields, which demonstrates the control potentialities offered by this system. For low optical depths, proper control with no phase modification along propagation may be performed. For arbitrarily higher optical depths, both the driving fields and the phase accumulated by the probe field along its propagation are affected which drastically modified the behavior of the system. Previous works on co-propagating control and probe field schemes have already showed new interesting phenomena like phase saturation and transparency [16]. This paves the way to further investigations for the present stationary control field configuration. Numerical simulations also showed a strong increase of the reflection and transmission factors with the optical depth. The combination of these effects offers a stimulating motivation for further study of this case.

ACKNOWLEDGMENTS

This research was funded in part by l'Agence Nationale de la Recherche (ANR), Project ANR-22-CE47-0011. For the purpose of open access, the authors have applied a CC-BY public copyright licence to any Author Accepted Manuscript (AAM) version arising from this submission.

-
- [1] K.-J. Boller, A. Imamoglu, and S. E. Harris, Phys. Rev. Lett. **66**, 2593 (1991).
 - [2] M. O. Scully, Phys. Rev. Lett. **67**, 1855 (1991).
 - [3] L. V. Hau et al., Nature (London) **397**, 594 (1999); M. M. Kash, V. A. Sautenkov, A. S. Zibrov, L. Hollberg, G. R. Welch, M. D. Lukin, Y. Rostovtsev, E. S. Fry, and M. O. Scully, Phys. Rev. Lett. **82**, 5229 (1999); L. J. Wang, A. Kuzmich and A. Dogarlu, Nature (London) **406**, 277 (2000); P. W. Millonni, Fast Light, Slow Light and Left-Handed Light, Taylor & Francis, New York, 2005.
 - [4] J. B. Pendry, Phys. Rev. Lett. **85**, 3966 (2000); R. A. Shelby, D. R. Smith, S. Shultz, Science **292**, 77 (2001)
 - [5] J. D. Joannopoulos, S. G. Johnson, J. N. Winn, R. D. Meade, Photonic Crystals: Molding The Flow Of Light, Princeton University Press, 2008.
 - [6] A. M. Herkommer, W. P. Schleich, and M. S. Zubairy, J. Mod. Opt. **44**, 2507 (1997) ; K. S. Johnson, J. H. Thywissen, N. H. Dekker, K. K. Berggren, A. P. Chu, R. Younkin, and M. Prentiss, Science **280**, 1583 (1998) ; S. Qamar, S.-Y. Zhu, and M. S. Zubairy, Phys. Rev. A **61**, 063806 (2000) ; V. Ivanov and Y. Rozhdestvensky, Phys. Rev. A **81**, 033809 (2010).
 - [7] A. André, M. D. Lukin, Phys. Rev. Lett. **89**, 143602 (2002) ; M. Bajcsy, A. S. Zibrov, M. D. Lukin, Nature **426**, 638 (2003) ; A. André, M. Bajcsy, A. S. Zibrov, and M. D. Lukin Phys. Rev. Lett. **94**, 063902 (2005).
 - [8] X. M. Su and B. S. Ham, Phys. Rev. A **71**, 013821 (2005) ; M. Artoni and G. C. La Rocca, Phys. Rev. Lett. **96**, 073905 (2006) ; Q.-Y. He, Y. Xue, M. Artoni, G. C. La Rocca, J.-H. Xu and J.-Y. Gao, Phys. Rev. B **73**, 195124 (2006) ; Q.-Y. He, J.-H. Wu, T.-J. Wang, and J.-Y. Gao, Phys. Rev. A **73**, 053813 (2006) ; J.-H. Wu, A. Raczynski, J. Zaremba, S. Zielińska-Kaniasty, M. Artoni and G.C. La Rocca, Journal of Modern Optics **56**, 768 (2009) ; K. Słowik, A. Raczynski, J. Zaremba, S. Zielińska-Kaniasty, M. Artoni and G.C. La Rocca, Journal of Modern Optics **58**, 978 (2011).
 - [9] Q. Jiang, Y. Zhang, D. Wang, S. Ahrens, J. Zhang, and S. Zhu, Opt. Express **24**, 24451 (2016).
 - [10] V. G. Arkhipkin, and S. A. Myslivets, Opt. Lett. **39**, 3223 (2014) ; V. G. Arkhipkin and S. A. Myslivets, Phys. Rev. A **93**, 013810 (2016) ; V. G. Arkhipkin, and S. A. Myslivets, J. Opt. **19**, 055501 (2017).

- [11] L. E. E. de Araujo, *Opt. Lett.* **35**, 977 (2010)
- [12] K. Słowik, A. Raczynski, J. Zaremba, S. Zielinska-Kaniasty, M. Artoni and G. C. La Rocca, *Phys. Scr. T***143**, 014022 (2011) ; Yihong Qi, Yueping Niu, Fengxue Zhou, Yandong Peng and Shangqing Gong, *J. Phys. B: At. Mol. Opt. Phys.* **44**, 085502 (2011).
- [13] Tao Li, Hailin Wang, N.H. Kwong, and R. Binder, *Opt. Express* **11**, 3298-3303 (2003).
- [14] J. C. Delagnes and M. A. Bouchene, *Phys. Rev. Lett.* **98**, 053602 (2007) ; J. C. Delagnes and M. A. Bouchene, *Phys. Rev. A* **76**, 045805 (2007) ; J. C. Delagnes and M. A. Bouchene *Phys. Rev. A* **76**, 053809 (2007).
- [15] F. A. Hashmi and M. A. Bouchene, *Phys. Rev. A* **77**, 051803(R) (2008).
- [16] F. A. Hashmi and M. A. Bouchene, *Phys. Rev. Lett.* **101**, 213601 (2008).
- [17] J. Wu, X.-Y. Lu and L.-L. Zheng, *J. Phys. B: At. Mol. Opt. Phys.* **43**, 161003 (2010) ; L. E. Zohravi, A. Vafafard, M. Mahmoud, *Journal Of Luminescence* **151**, 11 (2014).
- [18] S. H. Asadpour, H. Rahimpour Soleimani, *Optics Communications* **315**, 394 (2014) ; P. Kumar and S. Dasgupta, *J. Phys. B: At. Mol. Opt. Phys.* **47**, 175501 (2014) ; Ziauddin, Y.-L. Chuang, R.-K. Lee and S. Qamar, *Laser Phys.* **26**, 015205 (2016).
- [19] M. A. Anton and F. Carreno, *J. Opt.* **12**, 104006 (2010).
- [20] L. Yun, W. Pu, and P. Shuang-Yan, *Chin. Phys. B* **22**, 104203 (2013).
- [21] A. Vafafard and M. Sahrai, *JOSA B* **35**, 2118 (2018).
- [22] L. Jin, Y. Niu, and S. Gong, *Phys. Rev. A* **83**, 023410 (2011).
- [23] D. A. Smail et al, *Laser Phys. Lett.* **20**, 086003 (2023).
- [24] Z. Zhu, W.-X. Yang, X.-T. Xie, S. Liu, S. Liu, and R.-K. Lee, *Phys. Rev. A* **94**, 013826 (2016) ; D. Shah, U. Wahid, S. M. Arif, S. Muhammad, H. Ahmad, *Optical and Quantum Electronics* **54**, 360 (2022).
- [25] I. S. Gradshteyn and I. M. Ryzhik, *Table of integrals series and products*, Elsevier, 2014.